

## Polarization of $Y(nS)$ at the Fermilab Tevatron

Eric Braaten

*Physics Department, Ohio State University, Columbus, Ohio 43210*

Jungil Lee

*Deutsches Elektronen-Synchrotron DESY, D-22603 Hamburg, Germany*

(Received 18 December 2000; published 6 March 2001)

The polarization of inclusive  $Y(nS)$  at the Fermilab Tevatron is calculated within the nonrelativistic QCD factorization framework. We use a recent determination of the NRQCD matrix elements from fitting the CDF data on bottomonium production from run IB of the Tevatron. The result for the polarization of  $Y(1S)$  integrated over the transverse momentum bin  $8 < p_T < 20$  GeV is consistent with a recent measurement by the CDF Collaboration. The transverse polarization of  $Y(1S)$  is predicted to increase steadily for  $p_T$  greater than about 10 GeV. The  $Y(2S)$  and  $Y(3S)$  are predicted to have significantly larger transverse polarizations than  $Y(1S)$ .

DOI: 10.1103/PhysRevD.63.071501

PACS number(s): 13.85.Ni, 14.40.Gx

The production of heavy quarkonium provides an ideal testing ground for our understanding of the production mechanisms for heavy quarks and the nonperturbative QCD effects that bind the heavy-quark–antiquark pair into quarkonium. The purely leptonic decays of the  $J^{PC} = 1^{--}$  quarkonium states allow very clean measurements of their cross sections. One observable that is particularly sensitive to both the heavy-quark production mechanisms and the QCD binding effects is the polarization of the  $J^{PC} = 1^{--}$  states, which can be measured from the angular distribution of the leptons from their decays.

The nonrelativistic QCD (NRQCD) factorization approach provides a systematic framework for calculating the inclusive production rates of heavy quarkonium [1]. It is based on organizing the inclusive production rate into a double expansion in powers of  $\alpha_s(m_Q)$ , the running coupling constant at the scale of the heavy-quark mass, and of  $v_Q$ , the typical relative velocity of the heavy quark in the quarkonium rest frame. It should therefore be more reliable for bottomonium than for charmonium, because both of the expansion parameters  $\alpha_s(m_Q)$  and  $v_Q$  are smaller. In the NRQCD factorization approach, the larger-than-expected cross sections observed at hadron colliders are explained by introducing phenomenological parameters that describe the probabilities for the formation of the quarkonium state from color-octet heavy-quark–antiquark pairs [2]. Once those parameters are determined, the cross sections for polarized states are predicted without any additional parameters.

The most dramatic prediction that has emerged from the NRQCD framework is that in hadron colliders  $J^{PC} = 1^{--}$  quarkonium states should become increasingly transversely polarized as the transverse momentum  $p_T$  increases [3,4]. Quantitative predictions of the polarization of the charmonium states  $J/\psi$  and  $\psi(2S)$  at the Fermilab Tevatron indicate that there should be little polarization for  $p_T$  around 5 GeV, but that the transverse polarization should increase steadily at larger  $p_T$  [5–7]. The first measurements of the polarization of  $J/\psi$  and  $\psi(2S)$  by the Collider Detector at Fermilab (CDF) Collaboration [8] have shown no evidence for this

predicted increase. However, the discrepancies with the theoretical predictions are significant only in the highest  $p_T$  bin, so a definitive conclusion must await the higher statistics measurements that will be possible in run II of the Tevatron.

The CDF Collaboration has recently measured the polarization of inclusive  $Y(1S)$  in run IB of the Tevatron [9]. The results for the  $p_T$  bins from 2 to 20 GeV and from 8 to 20 GeV are both consistent with no polarization. Since the cross section falls rapidly with  $p_T$ , this indicates that there is little if any polarization for  $p_T$  below about 10 GeV. To determine whether this result is compatible with the NRQCD prediction, we need a quantitative calculation of the polarization for *inclusive*  $Y(1S)$  mesons.

The theoretical ingredients needed to calculate the polarization of direct  $Y(1S)$  mesons have been available for several years [6,10]. They were used by Beneke and Krämer and by Leibovich to predict the polarization of prompt  $\psi(2S)$  at the Tevatron [5,6]. The calculation of the polarization of inclusive  $Y(nS)$  is complicated by the fact that the inclusive signal includes  $Y(1S)$  mesons that come from decays of higher bottomonium states. Decays of  $\chi_b(1P)$ ,  $Y(2S)$ , and  $\chi_b(2P)$  account for about 27%, 11%, and 11% of the inclusive  $Y(1S)$  signal, respectively [11]. The missing ingredients in the calculation of the polarization of inclusive  $Y(1S)$  were the cross sections for polarized  $\chi_{bJ}$ . The necessary parton cross sections were recently calculated by Kniehl and Lee [12] and used to predict the polarization of prompt  $J/\psi$  at the Tevatron [7].

In this paper, we present quantitative predictions for the polarization of inclusive  $Y(1S)$ ,  $Y(2S)$ , and  $Y(3S)$  at the Tevatron using the NRQCD factorization formalism. We use NRQCD matrix elements for direct bottomonium production which were recently determined by Braaten, Fleming, and Leibovich from an analysis of data from run IB at the Tevatron [13]. Our result for the polarization of  $Y(1S)$  is consistent with the recent measurement by the CDF Collaboration in the  $p_T$  bin from 8 to 20 GeV. We predict that the transverse polarization of  $Y(1S)$  should increase steadily for  $p_T$

greater than about 10 GeV, and that the  $Y(2S)$  and  $Y(3S)$  should be even more strongly transversely polarized.

Since the  $Y(nS)$  is a spin-1 particle, the projection  $\lambda$  of its spin along any quantization axis should be  $-1$ ,  $0$ , or  $+1$ . The polarization of  $Y(nS)$  can be measured from the angular distribution of the leptons from its leptonic decays. The angular distribution of the positive lepton with respect to the  $Y(nS)$  momentum in the hadron center-of-momentum frame is proportional to  $1 + \alpha \cos^2 \theta$ , which defines the polarization variable  $\alpha$ . Taking the  $Y(nS)$  momentum in this frame to be the spin quantization axis, we define the longitudinally polarized  $Y(nS)$  to be the  $\lambda=0$  state and denote it by  $Y_L(nS)$ . The polarization variable  $\alpha$  is related to the fraction  $\xi$  of  $Y(nS)$  mesons that are longitudinally polarized by  $\alpha = (1 - 3\xi)/(1 + \xi)$ . The longitudinal polarization fraction  $\xi = \sigma_L/\sigma$  is the ratio of the inclusive cross section for  $Y_L(nS)$  to the inclusive cross section for  $Y(nS)$  summed over spins.

The cross section  $\sigma$  for inclusive  $Y(nS)$  is the sum of the direct cross section and the direct cross sections for the higher bottomonium states  $Y(mS)$  and  $\chi_b(mP)$  weighted by the inclusive branching fractions  $B_{H \rightarrow Y(nS)}$  for  $H \rightarrow Y(nS) + X$ :

$$\sigma[Y(nS)]_{\text{inc}} = \sigma[Y(nS)] + \sum_H B_{H \rightarrow Y(nS)} \sigma[H]. \quad (1)$$

For  $Y(3S)$ , we consider only the direct channel, neglecting any possible feeddown from higher states, such as  $\chi_b(3P)$ . For  $Y(2S)$ , we take into account the direct channel and the feeddown from  $\chi_b(2P)$  and  $Y(3S)$ . For  $Y(1S)$ , we take into account the direct channel and the feeddown from  $\chi_b(1P)$ ,  $Y(2S)$ ,  $\chi_b(2P)$ , and  $Y(3S)$ . The inclusive branching fractions  $B_{H \rightarrow Y(nS)}$  are given in Table I of Ref. [13].

The cross section  $\sigma_L$  for inclusive  $Y_L(nS)$  is the sum of the direct cross section for  $Y_L(nS)$  and the direct cross sections for the higher spin states  $Y(mS)_\lambda$  and  $\chi_{bJ}(mP)_\lambda$  weighted by  $B_{H \rightarrow Y(nS)}$  and the conditional probability  $P_{H_\lambda \rightarrow Y_L(nS)}$  for  $H_\lambda$  to decay into  $Y_L(nS)$  given that it decays into  $Y(nS)$ :

$$\begin{aligned} \sigma_L[Y(nS)]_{\text{inc}} &= \sigma[Y_L(nS)] \\ &+ \sum_{H,\lambda} B_{H \rightarrow Y(nS)} P_{H_\lambda \rightarrow Y_L(nS)} \sigma[H_\lambda]. \end{aligned} \quad (2)$$

The conditional probabilities are given in Table I. For  $\chi_{bJ}(nP)_\lambda \rightarrow Y_L(nS)$ ,  $n=1,2$ , they are given by simple angular-momentum factors for the radiative transition. For  $\chi_{bJ}(2P)_\lambda \rightarrow Y_L(1S)$  and  $Y(mS)_\lambda \rightarrow Y_L(nS)$ , we must average over the various decay paths weighted by their branching fractions. The important steps in the decay paths are of 3 kinds. The observed hadronic transitions  $Y(mS) \rightarrow Y(nS) + \pi\pi$  preserve the spin  $\lambda$ . For the radiative transitions  $\chi_{bJ}(2P)_\lambda \rightarrow Y_L(1S) + \gamma$  and  $Y(mS)_\lambda \rightarrow \chi_{bJ}(nP)_\lambda + \gamma$ , the probabilities for each spin state are given by simple angular-momentum factors [14]. Taking the weighted average over the decay paths, we obtain the results in Table I.

TABLE I. Conditional probabilities  $P_{H_\lambda \rightarrow Y_L(nS)}$  for the bottomonium spin state  $H_\lambda$  to decay into a longitudinally polarized  $Y(nS)$  given that it decays into  $Y(nS)$ .

$H$	$\lambda$	$Y(2S)$	$Y(1S)$
$Y(3S)$	0	$0.768 \pm 0.022$	$0.853 \pm 0.009$
	$\pm 1$	$0.116 \pm 0.011$	$0.073 \pm 0.005$
$\chi_{b2}(2P)$	0	$\frac{2}{3}$	$0.654 \pm 0.003$
	$\pm 1$	$\frac{1}{2}$	$0.494 \pm 0.001$
	$\pm 2$	0	$0.012 \pm 0.003$
$\chi_{b1}(2P)$	0	0	$0.013 \pm 0.003$
	$\pm 1$	$\frac{1}{2}$	$0.494 \pm 0.002$
$\chi_{b0}(2P)$	0	$\frac{1}{3}$	$\frac{1}{3}$
	$Y(2S)$	0	$0.941 \pm 0.009$
$\chi_{b2}(1P)$	$\pm 1$		$0.029 \pm 0.005$
	0		$\frac{2}{3}$
	$\pm 1$		$\frac{1}{2}$
$\chi_{b1}(1P)$	$\pm 2$		0
	0		0
	$\pm 1$		$\frac{1}{2}$
$\chi_{b0}(1P)$	0		$\frac{1}{3}$

The polarization variable  $\alpha$  for  $Y(nS)$  has been expressed as a ratio of linear combinations of the direct cross sections for  $Y(nS)$  and higher bottomonium states. The NRQCD factorization formula for the direct cross section for a bottomonium state  $H$  of momentum  $P$  and spin quantum number  $\lambda$  has the schematic form

$$d\sigma[p\bar{p} \rightarrow H_\lambda(P) + X] = \sum_n d\sigma[p\bar{p} \rightarrow b\bar{b}_n(P) + X] \langle O_n^{H_\lambda(P)} \rangle, \quad (3)$$

where the summation index  $n$  extends over all the color and angular momentum states of the  $b\bar{b}$  pair. The  $b\bar{b}$  cross section can be expressed as

$$d\sigma[p\bar{p} \rightarrow b\bar{b}_n(P) + X] = f_{i/p} \otimes f_{j/\bar{p}} \otimes d\hat{\sigma}[ij \rightarrow b\bar{b}_n(P) + X], \quad (4)$$

where  $f_{i/p}(x, \mu)$  and  $f_{j/\bar{p}}(x, \mu)$  are parton distribution functions (PDF's) and a sum over the partons  $i, j$  is implied. The parton cross sections  $d\hat{\sigma}$  can be calculated using perturbative QCD. All dependence on the state  $H$  is contained within the nonperturbative matrix elements  $\langle O_n^{H_\lambda(P)} \rangle$ . In general, they are Lorentz tensors that depend on the momentum  $P$  and the polarization tensor of  $H_\lambda$ . The Lorentz indices are contracted with those of  $d\sigma$  to give a scalar cross section. The symmetries of NRQCD can be used to reduce the tensor matrix elements  $\langle O_n^{H_\lambda(P)} \rangle$  to scalar matrix elements  $\langle O_n^H \rangle$  that are independent of  $P$  and  $\lambda$ . This reduces the variable  $\alpha$  to a ratio of linear combinations of the NRQCD matrix elements.

A nonperturbative analysis of NRQCD reveals how the various matrix elements scale with the typical relative veloc-

ity  $v$  of the heavy quarks. The most important matrix elements for the production of the  $S$ -wave states  $Y(nS)$  and  $\eta_b(nS)$  can be reduced to one color-singlet parameter  $\langle O_1^{Y(nS)}(^3S_1) \rangle$ , which scales like  $v^3$ , and three color-octet parameters  $\langle O_8^{Y(nS)}(^3S_1) \rangle$ ,  $\langle O_8^{Y(nS)}(^1S_0) \rangle$ , and  $\langle O_8^{Y(nS)}(^3P_0) \rangle$ , all of which scale like  $v^7$ . The most important matrix elements for the production of the  $P$ -wave states  $\chi_{bJ}(nP)$  and  $h_b(nP)$  can be reduced to a color-singlet parameter  $\langle O_1^{\chi_{b0}}(^3P_0) \rangle$  and a single color-octet parameter  $\langle O_8^{\chi_{b0}}(^3S_1) \rangle$ , both of which scale like  $v^5$ . At higher orders in  $v$ , so many new matrix elements enter that the predictive power of the NRQCD approach is lost. We therefore assume the matrix elements enumerated above are sufficient to describe the bottomonium cross sections.

The first determination of the color-octet matrix elements for bottomonium production was a pioneering analysis by Cho and Leibovich [15] of the data on bottomonium production from run IA of the Tevatron [16]. Because of the limited statistics, they had to use educated guesses for some of the matrix elements. An updated theoretical analysis based on the new CDF data from run IB [9] has been made by Braaten, Fleming, and Leibovich [13]. Their color-singlet matrix elements are given in Table II of Ref. [13]. Those for  $Y(nS)$  were determined phenomenologically from the leptonic decay rates of  $Y(nS)$ , while those for  $\chi_{bJ}(nP)$  were estimated from potential models. Their color-octet matrix elements are given in Table V of Ref. [13]. They were determined by fitting the CDF data on the differential cross sections for  $Y(1S)$ ,  $Y(2S)$ , and  $Y(3S)$  at  $p_T > 8$  GeV and from the fractions of  $Y(1S)$  from the decays of  $\chi_b(1P)$  and  $\chi_b(2P)$  [11].

The leading terms in the parton cross sections in Eq. (4) depend on the region of the transverse momentum  $p_T$  of the  $b\bar{b}$  pair. For  $p_T$  in the range  $8 \text{ GeV} < p_T < 30 \text{ GeV}$ , the leading terms are fusion contributions from the parton processes  $ij \rightarrow b\bar{b} + k$ . For  $p_T$  much greater than  $2m_b$ , fragmentation contributions from parton processes such as  $ij \rightarrow g + k$ , followed by  $g \rightarrow b\bar{b}$ , become important. For charmonium, fragmentation effects change the differential cross sections by less than 3% at  $p_T = 5$  GeV and less than 11% at  $p_T = 10$  GeV. Since  $m_b$  is 3 times larger than  $m_c$ , we expect fragmentation effects to change the differential cross sections for bottomonium by less than 11% for  $p_T$  less than 30 GeV. We will therefore avoid the complications of fragmentation by restricting our predictions to  $p_T < 30$  GeV.

For  $p_T$  much smaller than  $2m_b$ , parton processes such as  $ij \rightarrow b\bar{b} + ggg \dots$  involving the multiple emission of soft gluons become important and it is necessary to resum their effects. In the analysis of Ref. [13], this problem was avoided by using only the CDF data for  $p_T > 8$  GeV to fit the color-octet matrix elements. Since we will be using the matrix elements from that analysis, we will also restrict our predictions to  $p_T > 8$  GeV.

Having restricted our attention to the region  $8 \text{ GeV} < p_T < 30 \text{ GeV}$ , it should be safe to use only the fusion cross sections for  $d\hat{\sigma}$  in Eq. (4). We include the parton processes  $ij \rightarrow b\bar{b} + k$ , with  $i, j, k = g, q, \bar{q}$  and  $q = u, d, s, c$ . We treat the

$c$  quark as a massless parton. The leading-order parton cross sections  $d\hat{\sigma}$  are proportional to  $\alpha_s^3(\mu)$ . They are given in Refs. [6] and [10] for all the relevant  $b\bar{b}$  color and spin states with the exception of color-singlet  $^3P_J$  states, for which they are given in Ref. [12].<sup>1</sup>

We follow the analysis of Ref. [13] as closely as possible. We use a common renormalization and factorization scale  $\mu$  for  $f_{i/p}$ ,  $f_{j/\bar{p}}$ , and  $\alpha_s$ , taking its central value to be  $\mu_T = (m_b^2 + p_T^2)^{1/2}$  and allowing it to vary within the range  $\frac{1}{2}\mu_T$  to  $2\mu_T$ . We set  $m_b = 4.77 \pm 0.11$  GeV. We consider two choices for the PDF's for comparison: CTEQ5L and 1995 Martin-Roberts-Stirling-Thorne (MRST98) leading order (LO) sets [17]. We evaluate  $\alpha_s(\mu)$  from the one-loop formula with  $n_f = 5$  using the boundary conditions  $\alpha_s(M_Z) = 0.127$  for CTEQ5L and  $\alpha_s(M_Z) = 0.125$  for (MRST98) (LO). The cross section for direct  $Y(nS)$  depends on the linear combination  $\langle O_8(^1S_0) \rangle + r \langle O_8(^3P_0) \rangle / m_b^2$ , with  $r$  varying from 4.6 at  $p_T = 8$  GeV to 3.2 at  $p_T = 30$  GeV. In the cross section for direct  $Y_L(nS)$ ,  $r$  varies from 7.6 at  $p_T = 8$  GeV to 3.6 at  $p_T = 30$  GeV. We consider two extreme cases:  $\langle O_8(^1S_0) \rangle = 0$  and  $\langle O_8(^3P_0) \rangle = 0$ . The NRQCD matrix elements and their statistical errors are given in Tables II–V of Ref. [13]. The color-octet matrix elements in Table V of Ref. [13] also have an additional upper and lower error associated with changing  $\mu$  by a factor of 2. This allows the correlation between the errors in  $\mu$  and the color-octet matrix elements to be taken into account.

The polarization variable  $\alpha$  can be expressed as a ratio of linear combinations of NRQCD matrix elements. The errors in the matrix elements from Ref. [13] give large uncertainties in the numerator and the denominator, but they tend to cancel in the ratio. As our central value for  $\alpha$ , we take the average value from the 4 combinations corresponding to the two choices  $\langle O_8(^1S_0) \rangle = 0$  or  $\langle O_8(^3P_0) \rangle = 0$  and the two choices of PDF's. The deviations among the 4 combinations are included in our error. We compute the errors from the remaining parameters by varying each one independently for the choices (MRST98) (LO) and  $\langle O_8(^3P_0) \rangle = 0$  and using the central values of the other parameters. The parameters include the scale  $\mu$ , the mass  $m_b$ , 5 color-singlet matrix elements [13], 8 color-octet matrix elements [13], and 18 exclusive branching fractions for quarkonium transitions [18]. To compute the variation from  $\mu$ , we change  $\mu$  by a factor of 2 or  $\frac{1}{2}$  in the PDF's and in  $\alpha_s$  and simultaneously shift all the matrix elements by the second upper or lower error in Table V of Ref. [13]. This takes into account the large correlation between the choice of  $\mu$  and the values of the color-octet matrix elements. All the variations are added in quadrature to obtain the final error on  $\alpha$ .

Our results for the polarization variable  $\alpha$  for  $Y(1S)$ ,  $Y(2S)$ , and  $Y(3S)$  for the Tevatron at  $\sqrt{s} = 2.0$  TeV are shown as shaded bands in Figs. 1, 2, and 3, respectively. The

<sup>1</sup>There is a typographical error in Eq. (22) of Ref. [12]. The color-octet matrix elements  $\langle O_{Xc0}(^3S_1^{(8)}) \rangle = \langle O_8^{Xc0}(^3S_1) \rangle$  should be replaced by  $(2J+1) \langle O_{Xc0}(^3S_1^{(8)}) \rangle$ .

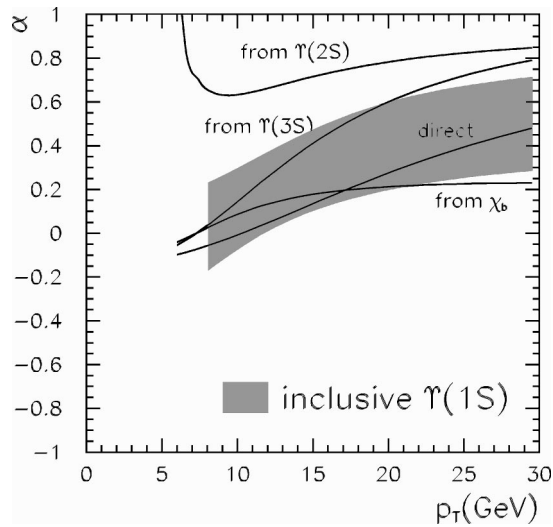


FIG. 1. Polarization variable  $\alpha$  vs  $p_T$  at  $\sqrt{s}=2.0$  TeV for inclusive  $Y(1S)$  (shaded band). The curves are the central values for direct  $Y(1S)$ ,  $Y(1S)$  from  $Y(2S)+\pi\pi$ , and  $Y(1S)$  from  $\chi_b(1P)+\gamma$  or  $\chi_b(2P)+\gamma$ .

curves in Figs. 1–3 are the central values of  $\alpha$  for direct  $Y(nS)$ , for  $Y(nS)$  from  $\chi_b(mP)+\gamma$ , and for  $Y(nS)$  from  $Y(mS)+\pi\pi$ . These channels together provide a complete decomposition of the inclusive rate. The fractions of the inclusive rate from each of these channels vary slowly with  $p_T$  and add up to 1. For inclusive  $Y(1S)$ , the fractions have been measured by the CDF Collaboration to be approximately 52% for direct  $Y(1S)$  and 27%, 11%, and 11% for  $Y(1S)$  from  $\chi_b(1P)$ ,  $Y(2S)$ , and  $\chi_b(2P)$ , respectively [11]. For inclusive  $Y(2S)$ , the fractions can be estimated from the analysis of Ref. [13] to be approximately 73% for direct  $Y(2S)$  and 25% and 2% for  $Y(2S)$  from  $\chi_b(2P)$  and  $Y(3S)$ , respectively. For  $Y(3S)$ , we ignored any possible feeddown from higher states.

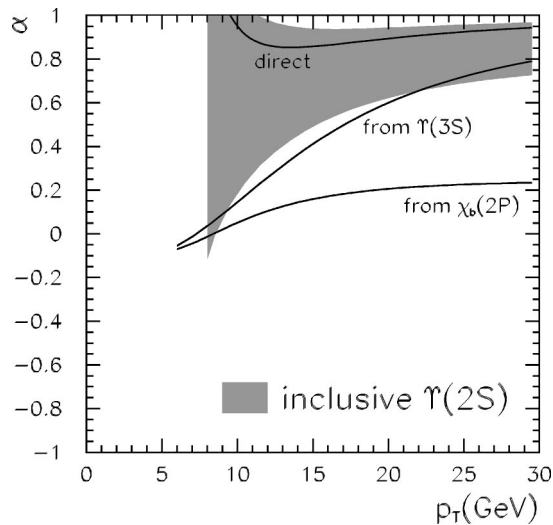


FIG. 2. Polarization variable  $\alpha$  vs  $p_T$  at  $\sqrt{s}=2.0$  TeV for inclusive  $Y(2S)$  (shaded band). The curves are the central values for direct  $Y(2S)$ ,  $Y(2S)$  from  $Y(3S)+\pi\pi$ , and  $Y(2S)$  from  $\chi_b(2P)+\gamma$ .

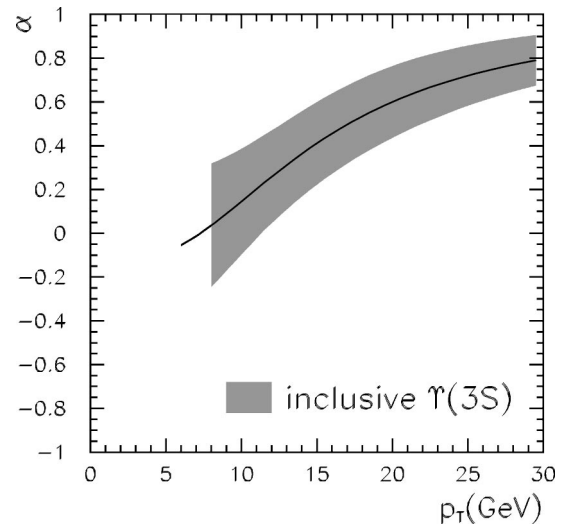


FIG. 3. Polarization variable  $\alpha$  vs  $p_T$  at  $\sqrt{s}=2.0$  TeV for  $Y(3S)$  (shaded band). The curve is the central value.

The predictions for  $\alpha$  for  $\sqrt{s}=1.8$  TeV are essentially identical to the predictions for  $\sqrt{s}=2.0$  TeV in Figs. 1–3. The cross sections  $\sigma_L$  and  $\sigma$  are both smaller by about 16%, but the change cancels in the ratio. Integrating over  $p_T$  in the range  $8 \text{ GeV} < p_T < 20 \text{ GeV}$ , we obtain  $\alpha = 0.13 \pm 0.18$ . This is in good agreement with the value measured by the CDF Collaboration:  $\alpha = 0.03 \pm 0.28$  [9].

In Figs. 1–3, the curves for  $\alpha$  for direct  $Y(nS)$  and for  $Y(nS)$  from  $Y(mS)+\pi\pi$  increase steadily with  $p_T$ . The curves for  $Y(nS)$  from  $\chi_b(mP)+\gamma$  increase at first, but then flatten out at a value of  $\alpha$  just above 0.2. Thus the feeddown from  $\chi_b(mP)$  tends to wash out the polarization. The fraction of  $Y(nS)$  from the  $\chi_b$  states is approximately 38% for  $n=1$ , 25% for  $n=2$ , and probably smaller yet for  $n=3$ . We therefore expect  $\alpha$  to increase more rapidly with  $p_T$  for  $Y(2S)$  and  $Y(3S)$  than for  $Y(1S)$ . A much larger transverse polarization for  $Y(2S+3S)$  than for  $Y(1S)$  has also recently been observed in bottomonium production in  $p$ - $Cu$  collisions at  $\sqrt{s}=38.8$  GeV [19].

The predictions in Figs. 1–3 are based on NRQCD matrix elements extracted from CDF data in the range  $8 \text{ GeV} < p_T < 20 \text{ GeV}$ . The extrapolation of these results to lower values of  $p_T$  should be considered unreliable. This is evident from the curves for direct  $Y(1S)$  from  $Y(2S)$  in Fig. 1 and direct  $Y(2S)$  in Fig. 2. The dramatic changes in these curves at the smaller values of  $p_T$  are artifacts of the fit of Ref. [13] having given negative central values for the color-octet matrix elements  $\langle O_8(^1S_0) \rangle$  or  $\langle O_8(^3P_0) \rangle$  for  $Y(2S)$ .

In run II of the Tevatron, the much higher statistics will allow more accurate measurements of the polarization of  $Y(1S)$  in several bins of  $p_T$ . It may also allow measurements of the polarizations of  $Y(2S)$  and  $Y(3S)$ . Significant improvements in the theoretical predictions are also possible. The most important improvement is taking into account the effects of multiple soft-gluon emission at low  $p_T$ . This would allow more accurate determinations of the color-octet matrix elements, since the entire  $p_T$  range of the CDF data

from run I could then be used in the fits. It is also important to include fragmentation effects, so that the predictions can be extrapolated with confidence to large  $p_T$ .

In conclusion, we have calculated the polarization of the  $\Upsilon(nS)$  states at the Tevatron using the NRQCD factorization approach. Our result is compatible with the recent CDF measurement for  $\Upsilon(1S)$  in the  $p_T$  bin from 8 to 20 GeV, which is consistent with no polarization. However, our results also

indicate that a nonzero transverse polarization should be observable for all three  $\Upsilon(nS)$  states in run II of the Tevatron.

J.L. thanks Sungwon Lee and Heuijin Lim for their useful advice. This work was supported in part by the U.S. Department of Energy Division of High Energy Physics under grant DE-FG02-91-ER40690 and by the KOSEF and the DFG through the German-Korean scientific exchange program DFG-446-KOR-113/137/0-1.

- 
- [1] G. T. Bodwin, E. Braaten, and G. P. Lepage, Phys. Rev. D **51**, 1125 (1995); **55**, 5853(E) (1997).  
 [2] E. Braaten and S. Fleming, Phys. Rev. Lett. **74**, 3327 (1995).  
 [3] P. Cho and M. B. Wise, Phys. Lett. B **346**, 129 (1995).  
 [4] M. Beneke and I. Z. Rothstein, Phys. Lett. B **372**, 157 (1996); **389**, 769(E) (1996).  
 [5] M. Beneke and M. Krämer, Phys. Rev. D **55**, 5269 (1997).  
 [6] A. K. Leibovich, Phys. Rev. D **56**, 4412 (1997).  
 [7] E. Braaten, B. A. Kniehl, and J. Lee, Phys. Rev. D **62**, 094005 (2000).  
 [8] CDF Collaboration, T. Affolder *et al.*, Phys. Rev. Lett. **85**, 2886 (2000).  
 [9] CDF Collaboration, R. Cropp, hep-ex/9910003; V. Papadimitriou, FERMILAB-Conf-00-308-E.  
 [10] M. Beneke, M. Krämer, and M. Vanttinen, Phys. Rev. D **57**, 4258 (1998).  
 [11] CDF Collaboration, T. Affolder *et al.*, Phys. Rev. Lett. **84**, 2094 (2000).  
 [12] B. A. Kniehl and J. Lee, Phys. Rev. D **62**, 114027 (2000).  
 [13] E. Braaten, S. Fleming, and A. K. Leibovich, Phys. Rev. D (to be published), hep-ph/0008091.  
 [14] P. Cho, M. B. Wise, and S. P. Trivedi, Phys. Rev. D **51**, 2039 (1995).  
 [15] P. Cho and A. K. Leibovich, Phys. Rev. D **53**, 150 (1996); **53**, 6203 (1996).  
 [16] CDF Collaboration, F. Abe *et al.*, Phys. Rev. Lett. **75**, 4358 (1997).  
 [17] A. D. Martin, R. G. Roberts, W. J. Stirling, and R. S. Thorne, Eur. Phys. J. C **4**, 463 (1998); CTEQ Collaboration, H. L. Lai *et al.*, *ibid.* **12**, 375 (2000).  
 [18] Particle Data Group, D. E. Groom *et al.*, Eur. Phys. J. C **15**, 1 (2000).  
 [19] Fermilab E866/NuSea Collaboration, C. N. Brown *et al.*, hep-ex/0011030.